On-demand gelation of ionic liquids using photoresponsive organometallic gelators

Sumitani, Ryo
Yamanaka, Masamichi
Mochida, Tomoyuki

(Citation)
Soft Matter,18(18):3479-3486

(Issue Date)
2022-05-14

(Resource Type)
journal article

(Version)
Accepted Manuscript

PAPER

On-demand Gelation of Ionic Liquids Using Photoresponsive Organometallic Gelators†

Received 00th January 20xx,
Accepted 00th January 20xx

DOI: 10.1039/x0xx00000x

Ryo Sumitani,[a] Masamichi Yamanaka [b] and Tomoyuki Mochida *[a,c]

The reversible formation of ionic liquid gels, or ionogels, upon external stimuli could improve their versatility and expand their application scope in electronic, biomedical, and micro-engineering systems. Herein, we developed organometallic compounds that release low-molecular-weight gelators upon photoirradiation, which facilitate the on-demand photogelation of ionic liquids (ILs). The chemical formulae of the gelator-coordinated complexes are [Ru(C_5H_5)**L**]X (**L** = $C_6H_5NHCONHC_{12}H_{25}$; X = PF_6, $B(CN)_4$). Each of the complexes were ILs that are easy to synthesize and miscible in ILs. By adding a small amount of the complex, various ILs were transformed to gels upon UV photoirradiation. The PF_6 salt allowed the photogelation of ILs with coordinating substituents, whereas the $B(CN)_4$ salt allowed the photogelation of non-coordinating ILs, albeit the reaction was slower. These gels underwent the reverse reaction and liquefied back when heated, and the photogelation was repeatable for ILs with coordinating cations.

Introduction

Supramolecular gels, also called physical gels, are viscoelastic materials that are typically formed by adding low-molecular-weight gelators (LMWGs) to solvents such as water, organic solvents, and ionic liquids (ILs).[1–4] LMWGs undergo self-assembly through intermolecular interactions such as hydrogen bonding, electrostatic interactions, π–π stacking, and van der Waals interactions to form three-dimensional fibril networks, resulting in gelation.[5,6] They are versatile and can be used as separators,[7] emulsifiers,[8,9] and absorbents[10,11] and in catalytic reactions[12–14] and tissue engineering.[15,16]

In recent years, various stimuli-responsive LMWGs have been developed, which facilitate gelation of water or organic solvents by the application of light,[17] heat,[15,18,19] pH,[10,11,20] chemical stimulus,[21,22] and enzymes.[23,24] In particular, photo-induced gel formation is useful for non-contact, non-invasive gelation control. There are several examples of reversible gelation by using photoisomerizable LMWGs, polymer gelators, or metallogelators, typically containing azobenzene moieties.[17,25,26] The LMWGs with photocleavable gelation inhibitor sites, such as *o*-nitrophenyl and coumarin, exhibit gelation capability upon photoirradiation, though they are irreversible.[27–29] In addition to photo-stimuli, enzymatic reactions[30–33] and Diels-Alder reactions[18,19] have been used for gelation control via the cleavage of inhibitor sites.

Ionogels, formed by the gelation of ILs, are highly useful for applications as solid electrolytes, actuators, and gas separation membranes[4,34–36] owing to their high ionic conductivity and non-volatility.[37] Photogelation of ILs could extend their manipulation modes and applications, though this remains a challenge; there are only a few examples of IL photogelation, which use specially designed polymer gelators.[38–43] In comparison with polymer gelators, LMWGs are useful because only a small amount is required for gelation (favorable for ionic conductivity) and they are easily modified and manipulated. There are several LMWGs that are useful for the gelation of ILs, which are typically benzene derivatives with urea substituents.[44,45] Therefore, we aimed to develop a unique, versatile method for the on-demand photogelation of ILs using such LMWGs. For this purpose, we developed organometallic compounds that release LMWGs upon photoirradiation in ILs.

The structures of the gelator-coordinated sandwich complexes designed by us, [CpRu**L**]X (**1-X**, X = PF_6, $B(CN)_4$; Cp = C_5H_5, **L** = $PhNHCONHC_{12}H_{25}$), and their gelator release mechanisms are shown in Fig. 1a. Note that **1-X** are salts; thus, they are miscible in ILs. The complex releases gelator molecule **L** upon UV photoirradiation, and the reverse reaction occurs upon heating. Herein, we chose an LMWG (**L**) suitable for the gelation of ILs.[45,46] This reaction, which proceeds in the presence of coordinating molecules, is based on the reactivity of Ru sandwich complexes in coordinating solvents, as shown in Fig. 1b.[47,48] We previously developed several photoreactive ILs using this mechanism.[49–53] As shown in Fig. 1c, after the addition of a small amount of **1-X**, various ILs transformed to ionogels upon UV irradiation. These gels underwent the reverse reaction and liquefied back when heated, and the photogelation was repeatable for ionic liquids with coordinating cations. Photogelation of organic solvents was also investigated.

[a]*Department of Chemistry, Graduate School of Science, Kobe University, 1-1 Rokkodai, Nada, Kobe, Hyogo 657-8501, Japan.*
E-mail: tmochida@platinum.kobe-u.ac.jp
[b]*Meiji Pharmaceutical University, 2-522-1 Noshio, Kiyose, Tokyo 204–8588, Japan*
[c]*Research Center for Membrane and Film Technology, Kobe University, 1-1 Rokkodai, Nada, Kobe, Hyogo 657-8501, Japan*

†Electronic Supplementary Information (ESI) available: DSC curves, FT-IR spectra, ^{1}H NMR spectra, photographs, SEM images, dynamic viscoelastic measurements, crystal structures, TG-DTA curves. See DOI: 10.1039/x0xx00000x

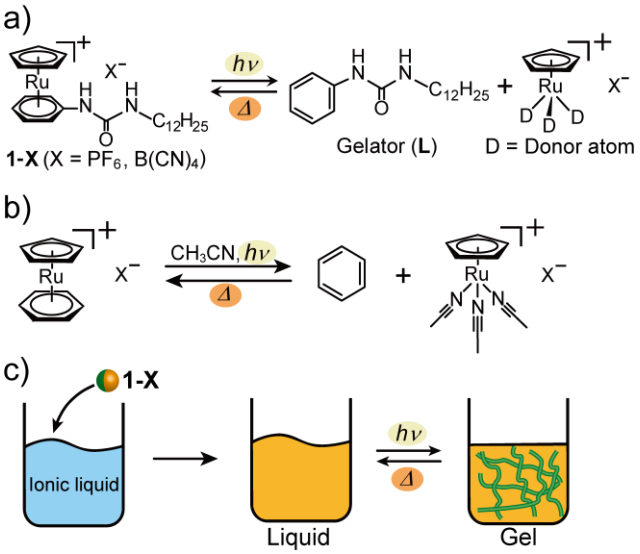

Fig. 1. (a) Photochemical release of low-molecular-weight gelator **L** from gelator-coordinated complexes **1-X** (X = PF_6, $B(CN)_4$) designed in this study. In the figure, D is the donor atom of the coordinating molecule in the liquid. (b) Photochemical and thermal reversible reactions of cationic sandwich-type Ru complexes in acetonitrile.[47,48] (c) Schematic representation of a reversible ionogel formation upon the application of light and heat after addition of **1-X**.

Experimental

General

$C_6H_5NHCONHC_{12}H_{25}$ (**L**),[45] *o*-$C_6H_4(CH_2Ph)(NHCONHC_{12}H_{25})$ (**L'**),[44] [C_3CNmIm][FSA],[54] and [BmIm][$B(CN)_4$][55] were synthesized according to previously reported methods. [C_6CNEt_3N][Tf_2N] was synthesized by using a standard method (ESI†), and [BmIm][PF_6] was purchased from Kokusan Chemical Co., Ltd. (Japan). Other reagents were purchased from TCI Co. (Japan). ^{1}H and ^{19}F NMR spectra were recorded using a Bruker Avance 400 spectrometer. FT-IR spectra were measured using a Thermo Nicolet iS5 system with an attenuated total reflection (ATR) attachment. Elemental analyses were performed using a PerkinElmer 2400II elemental analyzer. DSC was performed using a TA Instruments Q100 differential scanning calorimeter at a sweep rate of 10 °C min^{-1}. Dynamic viscoelasticity was measured using a TA Instruments DHR-1 rheometer equipped with an 8-mm parallel plate. The frequency dependence of the dynamic viscoelasticity was determined at 25 °C. A Hamamatsu LC-L1V3 Lightning Cure UV-LED light source (LED lamp, wavelength: 365 nm, intensity: 650 mW cm^{-2}) was used for UV photoirradiation. The ratio of photodissociated cations was determined from the ^{1}H NMR spectra (CD_3CN). SEM was performed on a Hitachi High-Technologies Miniscope TM4000 or JEOL JSM-5510 system.

Synthesis of [CpRu(L)][PF_6] (1-PF_6)

Under a nitrogen atmosphere, ligand **L** (42 mg, 0.14 mmol) was added to a solution of [$CpRu(CH_3CN)_3$]PF_6 (50 mg, 0.12 mmol) in 1,2-dichloroethane (2.5 mL) and stirred at 90 °C for 21 h. The resultant solution was evaporated under reduced pressure, and the residue was purified by column chromatography (alumina, eluent: acetonitrile). The recrystallization of the product from acetone–diethyl ether (−40 °C) produced colorless needle-like crystals (37 mg, 51%). ^{1}H NMR (400 MHz, CD_3CN): δ = 0.91 (t, 3H, *CH*$_3$, *J* = 7.01 Hz), 1.29–1.36 (m, 18H, $NHC_2H_4C_9H_{18}CH_3$), 1.49 (m, 2H, $NHCH_2CH_2$), 3.16 (q, 2H, $NHCH_2$, *J* = 5.92 Hz), 5.27 (s, 5H, Cp-*H*$_5$), 5.46 (m, 1H, $NHC_{12}H_{25}$), 5.86 (t, 1H, Ar-*H*, *J* = 5.58 Hz), 6.02 (dd, 2H, Ar-*H*, *J* = 0.91, 6.49 Hz), 6.63 (dd, 2H, Ar-*H*, *J* = 5.98, 6.29 Hz), 7.20 (m, 1H, PhN*H*). FT-IR (ATR, cm^{-1}):556 (P–F), 824 (P–F), 1238, 1299, 1363, 1393, 1406, 1417 (Cp, C=C), 1465, 1528, 1573 (Arene, C=C), 1667 (C=O), 2849, 2918, 2956, 3125 (C–H). Anal. Calcd. for $C_{24}H_{37}F_6N_2OPRu$: C, 46.83, H, 6.06, N, 4.55. Found: C, 47.14, H, 6.32, N, 4.54.

Synthesis of [CpRu(L)][$B(CN)_4$] (1-$B(CN)_4$)

A solution of **1-PF_6** (46 mg, 0.073 mmol) in a mixture of acetonitrile (0.1 mL) and methanol (1 mL) was charged to an anion exchange column (Dowex 1X8-100, chloride form, 7 g) and eluted with methanol (100 mL). The eluent was concentrated under reduced pressure and the anion-exchange procedure was repeated. The complete exchange of the anion was confirmed by the absence of the PF_6 peak (δ = −73.83, −71.92) in the ^{19}F NMR spectrum (solvent: CD_3CN). Chloride salt was obtained quantitatively as a pale-yellow liquid; the product was vacuum-dried at ambient temperature for 3 h. K[$B(CN)_4$] (23 mg, 0.15 mmol) was added to a mixture of water (10 mL), acetone (1 mL), and chloride salt and stirred for 10 min. Acetone was then evaporated under reduced pressure; water and dichloromethane were added to the residue. The residue was extracted five times with dichloromethane, and the organic layer was combined and washed three times with water. The organic layer was then dried over anhydrous magnesium sulfate. After solvent evaporation, the residue was dried under vacuum for 5 h at 70 °C. A silver nitrate solution was used to verify the absence of chloride ions. The desired product was obtained as a pale-yellow liquid (78 mg, 94%). ^{1}H NMR (400 MHz, CD_3CN): δ = 0.91 (t, 3H, *CH*$_3$, *J* = 7.01 Hz), 1.29–1.36 (m, 18H, $NHC_2H_4C_9H_{18}CH_3$), 1.49 (m, 2H, $NHCH_2CH_2$), 3.16 (q, 2H, $NHCH_2$, *J* = 5.92 Hz), 5.27 (s, 5H, Cp-*H*$_5$), 5.46 (m, 1H, $NHC_{12}H_{25}$), 5.86 (t, 1H, Ar-*H*, *J* = 5.58 Hz), 6.02 (dd, 2H, Ar-*H*, *J* = 0.91, 6.49 Hz), 6.63 (dd, 2H, Ar-*H*, *J* = 5.98, 6.29 Hz), 7.20 (m, 1H, PhN*H*). FT-IR (ATR, cm^{-1}): 842, 932, 1226, 1295, 1462 (Cp, C=C), 1524, 1563 (Arene, C=C), 1682 (C=O), 2222 (CN). Anal. Calcd. for $C_{28}H_{37}BN_6ORu$: C, 57.44, H, 6.37, N, 14.35. Found: C, 57.36, H, 6.29, N, 14.24.

Gelation Experiments

A small amount (1 mg, 5 wt.%) of **1-PF_6** or **1-$B(CN)_4$** was added to each ionic liquid (20 mg) on a glass plate, which was then heated at 120 °C and allowed to cool to ambient temperature. The UV photoirradiation experiments were conducted in a glove box filled with argon using samples placed on a cooling plate maintained at 10 °C. The thermal reactions of the samples were carried out at 120 °C in the glove box.

The dissociation rates of the cations in the photoproducts were determined from the ratio of [$CpRu(CD_3CN)_3$]$^+$ and the remaining sandwich complex in the ^{1}H NMR spectra (CD_3CN). Photogelation of organic solvents was investigated by adding 5 wt.% of **1-PF_6**, **1-**

B(CN)$_4$, or **2-B(CN)$_4$** to the solvents in screw vials, which were flushed with nitrogen. The vials were placed on a cooling plate maintained at 10 °C and UV light was irradiated from outside the vials. The ionogels prepared by adding gelator **L** (2.4–2.5 wt.%) to the ILs, were used as the reference gels after being heated up to 120 °C and cooled down to room temperature.

X-ray Crystallography

Single crystals of **1-PF$_6$**, suitable for structural analysis, were grown by recrystallization from acetone–diethyl ether by slow cooling to −40 °C. The X-ray diffraction data were collected using a Bruker APEX II Ultra diffractometer (X-ray source: MoKα) and the calculations were performed using SHELXL.[56] The crystallographic parameters are listed in Table S1. CCDC 2121035 contains the crystallographic data for this compound. These data can be obtained free of charge via www.ccdc.cam.ac.uk/data_request/cif.

Result and discussion

Synthesis and Properties of Photoresponsive Gelators

Salt **1-PF$_6$** was obtained as a white solid with a melting point of 90 °C by the reaction of [CpRu(CH$_3$CN)$_3$]PF$_6$ with gelator **L**. Upon cooling from the melt, the salt underwent a glass transition at 8°C (Fig. S1, ESI†). Salt **1-B(CN)$_4$** was obtained as a pale-yellow liquid via anion exchange from **1-PF$_6$**. This liquid did not crystallize upon cooling and underwent a glass transition at −36 °C. Both salts are regarded as ILs with melting points below 100 °C.

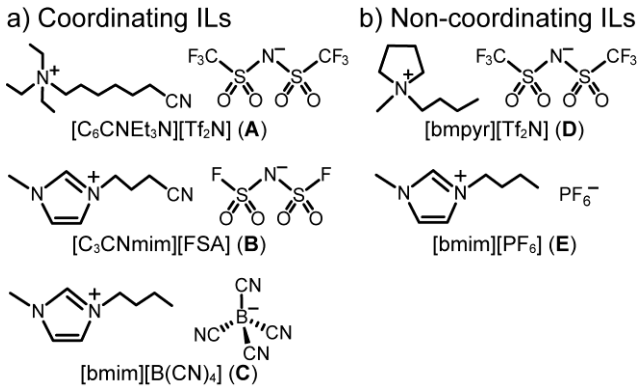

Fig. 2. Structures of (a) coordinating and (b) non-coordinating ILs used for gelation experiments.

Table 1. Typical experimental conditions for photogelation and gel–sol transition temperatures of the resultant gels.

Gelator	Medium	Photoirradiation time	Heating time[a]	T_{gel} (°C)[b]	
				heating	cooling
1-PF$_6$	**A**	4 h	10 min	73	5
	B	4 h	10 min	83	55
	C	4 h	4 h[c]	57	28
	E	no reaction			
1-B(CN)$_4$	**D**	18 h	1 h[c]	77	49
	E	18 h	1 h[c]	85	55

[a] Heated at 120 °C. [b] Determined by DSC (1st cycle, scan rate 10 °C min^{-1}). [c] Partial decomposition of the gelator occurred during heating.

The addition of a small amount (5 wt.%) of these salts to ILs **A–E**, shown in Fig. 2, resulted in the formation of homogeneous liquids except for **B**. Salt **1-PF$_6$** was less soluble in **B** and stayed as a suspension at room temperature. However, the solubility of **1-PF$_6$** increased at higher temperatures; it formed a homogeneous solution at 80 °C. These results show that the gelation capability of **L** is lost when it is coordinated to the CpRu unit, though **L** can gelate these ILs. The photogelation of the ILs after adding **1-X** was then investigated, as summarized in Table 1, the details are described in the following sections.

Photogelation of Coordinating ILs with 1-PF$_6$

After adding a small amount of **1-PF$_6$**, the ILs containing cyano groups in the cation or anion underwent gelation upon photoirradiation, and the gels liquefied again upon heating. However, the non-coordinating ILs did not form gels under the same conditions.

[C$_6$CNEt$_3$N][Tf$_2$N] (**A**) and [C$_3$CNmim][FSA] (**B**), which contained 5 wt.% of **1-PF$_6$**, were a pale-yellow liquid and a white suspension, respectively. A small amount of undissolved **1-PF$_6$** remained in the latter. The gelator was released from the complexes upon 4 h of UV photoirradiation (365 nm, LED), and the ILs transformed to yellow gels (Fig. 3a). In **B**, the undissolved complex gradually dissolved during photoirradiation. The products maintained the gel state after being maintained at room temperature for a week. Upon heating to 120 °C, the gels

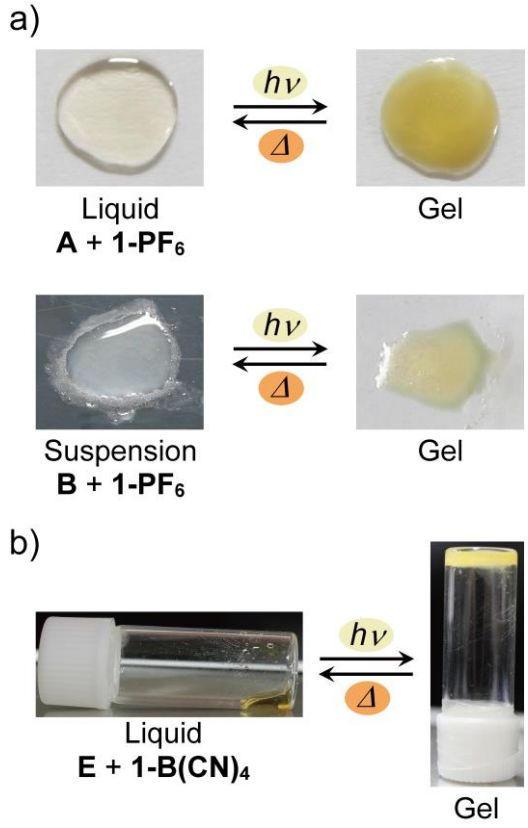

Fig. 3. Photographs of (a) **A**, **B**, and (b) **E** (containing 5 wt.% **1-X**) before and after photoirradiation.

underwent quantitative reverse reactions within 10 min, returning to the pale-yellow liquid and suspension states. The thermal reverse reaction occurred within a short time period because the resultant cation-coordinated Ru complexes easily dissociated. The photochemical and thermal reactions were repeated at least several times.

The structural changes of the Ru complexes upon photoirradiation were confirmed by ^{1}H NMR and FT-IR spectroscopy (Fig. 4 and Figs. S4 and S5, ESI†). The photorelease of the gelator in **B** was complete within 2 h, whereas the reaction rate in **A** was 84% at 2 h and ~90% at 4 and 6 h. The lower reaction rate in **A** may be ascribed to the occurrence of the concomitant thermal reverse reaction during photoirradiation, owing to the lower thermal stability of the resultant Ru complex (see below). In the FT-IR spectra, the peaks ascribed to the C=O stretching vibration of the gelator (1626 cm^{-1}) appeared after photoirradiation, confirming gelator release, though the change in the CN stretching vibration was not clear. Upon heating them, their spectra reverted to those before photoirradiation.

Similarly, the photogelation of [Bmim][B(CN)$_4$] (**C**), containing a cyano group in the anion, was possible upon the addition of **1-PF$_6$** (Fig. S3a, ESI†). Upon 4 h of photoirradiation, the gelation of the liquid occurred with quantitative gelator release. A small amount of anion-coordinated yellow Ru complexes was formed and suspended in the gel. Upon heating at 120 °C for 4 h, the resultant gel returned to a uniform liquid state, during which the gelator coordinated to the Ru complex. However, gelation did not occur upon further photoirradiation, unlike that in **A** and **B**. This is because partial decomposition (~30%) of the gelator occurred during the longer heating time. The reverse reaction for **C** took much longer than those for **A** and **B** because the anion-coordinated complex does not readily dissociate.

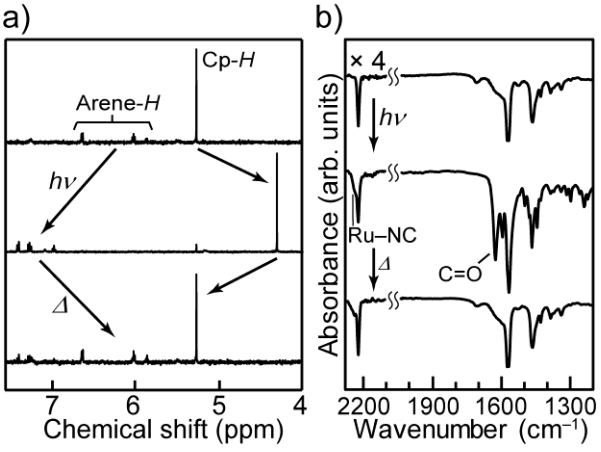

Fig. 4. (a) ^{1}H NMR spectra (in CD_3CN) of **A** (containing 5 wt.% **1-PF$_6$**) before and after photoirradiation for 4 h and after heating at 120 °C for 10 min. The Ru complex after the photochemical reaction was observed as the solvent-coordinated complex $[CpRu(CD_3CN)_3]^+$. (b) FT-IR spectra of **C** (containing 5 wt.% **1-PF$_6$**) before and after photoirradiation for 4 h and after heating at 120 °C for 4 h.

In the FT-IR spectrum of **C** after photogelation, the C=O stretching vibration peak of the released gelator (1626 cm^{-1}) and the CN stretching vibration peaks of the anion-coordinated Ru complex (2241 cm^{-1})[47,48] were observed (Fig. 4b). In **1-PF$_6$**, the C=O stretching vibration peak of the coordinated gelator appeared at 1667 cm^{-1} (Fig. S2a, ESI†), and the CN stretching vibration of the B(CN)$_4$ anion is IR silent because of its high symmetry.[50,57] Upon heating the gel, its spectrum became identical to that before its photoirradiation.

In contrast, photogelation did not occurr for [Bmim][PF$_6$] (**E**) containing 5 wt.% **1-PF$_6$**, which is ascribed to the absence of coordinating substituents that stabilize the Ru complex in the reaction scheme shown in Fig. 1a. The absence of gelator release was also confirmed through ^{1}H NMR spectroscopy.

These results demonstrate that the ILs with coordinating substituents in either the cation or anion can be photogelated with **1-PF$_6$** and the reaction can proceed even when the ILs are in a suspension state. It is convenient that the addition of only a small amount of the complex is sufficient for photogelation, and the gelation time would be shortened by the use of a high-power light source. The ILs containing cyano substituents exhibit suitable reaction solvent properties[58,59] and high CO_2 absorption capacity;[55,60,61] hence, the photogelation of such functional ILs would be useful for broadening their application scope.

Photogelation of Non-coordinating ILs with 1-B(CN)$_4$

The photogelation of non-coordinating ILs was achieved using **1-B(CN)$_4$** with the coordinating anion, though the reaction took longer.

Upon UV photoirradiation (365 nm, LED) for 18 h, pale-yellow liquids of [bmpyr][Tf$_2$N] (**D**) or [bmim][PF$_6$] (**E**) containing 5 wt.% of **1-B(CN)$_4$** transformed to yellow gels (Figs. 3b and S3b, ESI†). Although the gelator release was quantitative at 18 h, the reaction rate was still 66% at 4 h for **E**, requiring a significantly longer photoirradiation time than that required by the ILs described in the previous section. This happened because the anions in the liquids are mostly PF_6^-, making the reaction of the Ru complex with $B(CN)_4^-$ substantially less efficient. The release of the gelator upon photoirradiation and the coordination of the anion to the Ru ion were confirmed spectroscopically (Figs. S4 and S5, ESI†). The gels obtained via photoirradiation maintained their gel state even after remaining idle for a week. Upon heating at 120 °C for 1 h, the gels liquefied again owing to the reverse reaction. However, the gelation of the liquid did not occur upon further photoirradiation because the thermal reaction of the anion-coordinated complex involved partial decomposition of the gelator, similar to that in the gel containing **C**, as described in the previous section. The decomposition was facilitated at higher temperatures.

Structures and Properties of Ionogels Prepared via Photoirradiation

The structures and the thermal and mechanical properties of the ionogels were investigated by differential scanning calorimetry (DSC), scanning electron microscopy (SEM), and dynamic viscoelasticity measurements. The physical properties

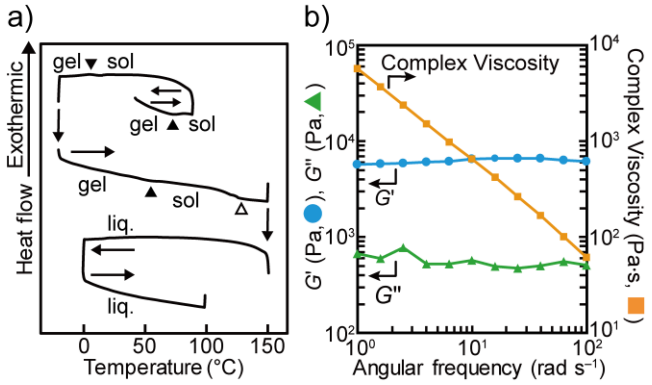

Fig. 5. (a) DSC curves of **A** (containing 5 wt.% **1-PF$_6$**) after photogelation, where liq. is a liquid state. The peaks corresponding to the gel–sol transition and gelator coordination are designated by ▲ and △, respectively. (b) Angular frequency dependence of storage modulus (G'), loss modulus (G''), and complex viscosity of **B** (containing 5 wt.% **1-PF$_6$**) after photogelation (25 °C, strain 0.1%).

Table 2. Storage modulus (G'), loss modulus (G''), and yield strain of ionogels prepared by photogelation[a)] and gelator addition[b)].

Medium	Gel preparation	Gelator	G' (Pa) [c)]	G'' (Pa) [c)]	Yield strain (%) [d)]
A	Photogelation	**1-PF$_6$**	1.5×10^2	6.1×10^1	0.2
	Photogelation + Heating[e)]	**1-PF$_6$**	7.3×10^3	7.0×10^2	0.4
	Gelator addition	**L**	1.1×10^4	3.7×10^3	0.1
B	Photogelation	**1-PF$_6$**	6.5×10^3	5.7×10^2	0.4
	Gelator addition	**L**	5.7×10^3	8.7×10^2	0.1
C	Photogelation	**1-PF$_6$**	7.6×10^3	1.1×10^3	0.4
	Photogelation + Heating[e)]	**1-PF$_6$**	2.4×10^5	3.2×10^4	0.4
	Gelator addition	**L**	1.3×10^5	1.5×10^4	0.1
D	Photogelation	**1-B(CN)$_4$**	1.3×10^4	2.0×10^3	0.1
	Gelator addition	**L**	1.5×10^4	3.6×10^3	0.1
E	Photogelation	**1-B(CN)$_4$**	1.9×10^4	2.2×10^3	0.4
	Gelator addition	**L**	7.0×10^3	6.3×10^2	0.3

a) Prepared upon photoirradiation after the addition of **1-X** (5 wt.%). b) Heated to 120 °C after the addition of gelator **L** (2.4–2.5 wt.%). c) Angular frequency 10 rad s^{-1}, strain 0.1%. d) Angular frequency 10 rad s^{-1}. e) Heated to 100 °C after photogelation.

of the gels prepared via photoirradiation were found to be comparable to those of the ionogels prepared by the addition of the gelator to the corresponding ILs. In some cases, additional thermal treatment after photogelation was conducted to allow the formation of stronger gelator networks.

The occurrence of thermal gel–sol transitions in the ionogels prepared via photogelation was detected through DSC. The transition temperature (T_{gel}, heating) ranged between 57 and 85 °C depending on the ILs (Table 1 and Fig. S6, ESI†). Except for the gel prepared from **1-PF$_6$** and **A** via photoirradiation, the sol–gel transition temperatures of the gels measured upon cooling (T_{gel}, cooling) were approximately 30 °C lower than those measured upon heating (T_{gel}, heating). Their gol-gel transition temperatures were almost the same as those of the gels prepared by the addition of gelator **L** to each IL (reference gels), showing similar hysteresis (Table S2, ESI†). Thermal hysteresis is often observed in physical gels.[62]

The DSC curves of the ionogel containing **A** are shown in Fig. 5a. The gel–sol transition was observed in the first cycle at 73 °C during heating, similar to the reference gel (T_{gel} = 70 °C, heating). However, the sol–gel transition was observed at 5 °C during cooling; the transition temperature was significantly lower than that of the reference gel (T_{gel} = 41 °C, cooling; Table S2, ESI†). This is probably owing to the partial thermal reverse reaction that occurred during the measurement, which reduced the gelator concentration. In the second cycle, the gel–sol transition was observed at 54 °C (T_{gel}, heating), which was lower than that in the first cycle owing to the same reason. The facile thermal reverse reaction is ascribed to the intramolecular repulsion between the ammonium cations in the photogenerated complex. Upon further heating the gel, a small, very broad endothermic peak was observed at ~130 °C, which corresponds to the coordination of the gelator to the CpRu unit,[49] after which the gel–sol transition peaks disappeared (Fig. 5a). The other ionogels prepared by photogelation exhibited almost the same thermal behavior, but the gel–sol transition were identical in the first and second cycles because the photogenerated complexes were thermally more robust. In the DSC curves of the ionogel containing **B**, small peaks corresponding to the dissolution (79 °C) and precipitation of **1-PF$_6$** were also observed after the thermal reverse reaction, as expected for the suspension.

The SEM image of the ionogels prepared via photogelation showed fibrous microcrystalline network structures consisting of bundled nanosticks (Fig. S7, ESI†). These are microcrystalline gels[63] although physical gels with LMWGs typically have linearly interconnected structures. Similar structures were observed in the gels prepared by the addition of gelator **L** to each IL (Fig. S7, ESI†).

The storage modulus (G') and loss modulus (G'') of the ionogels prepared via photogelation, as investigated by dynamic viscoelasticity measurements, are listed in Table 2. In all ionogels, G' was higher than G'' within the angular frequency range of 1–100 rad s^{-1} (strain 0.1%), indicating elastic behavior (Figs. 5b and S8a, ESI†). The complex viscosities decreased with increasing angular frequencies, which is a typical behavior of gels.[64] These were soft gels, which yielded at 0.1%–0.4% strain (Fig. S8b, ESI†). These gels exhibited almost the same viscoelastic modulus as the reference gels prepared with gelator **L**; however, the gels with **A** and **C** prepared via photogelation exhibited much lower values, which are ascribed to their higher gelator crystallinity. Thermal treatment (heated to 100 °C and subsequently cooled to ambient temperature) was effective for these gels in forming a stronger gelator network via the sol–gel transition (Table 2).

Photogelation of Organic Solvents

Salt **1-X** also allowed the photorelease of the gelator in organic solvents, producing gels under suitable conditions. The gelation capability could be modulated by changing the ligand species.

Upon UV photoirradiation for 1 h at 10 °C of a pale-yellow acetonitrile solution containing 5 wt.% **1-PF$_6$**, the Ru complex quantitatively released the gelator in the solution. Although no gelation occurred, given that the gelator precipitated as a white solid (Fig. 6a), the gel was formed by heating the mixture to 70 °C to dissolve the solid and subsequently cooling it to 25 °C. This is because the gelator network structure is formed through sol–gel transition. Upon heating the yellow gel at 120 °C for 20 min, the complex underwent a reverse reaction to give the original liquid; hence, the photogelation was repeatable. Similarly, a benzonitrile solution containing 5 wt.% **1-PF$_6$** changed from colorless to pale yellow upon 1 h of UV photoirradiation (Fig. 6b), during which the Ru complex quantitatively released the gelator in the solution. Although the resultant solution was liquid at ambient temperature owing to its low gel–sol transition temperature, it formed a gel within 1 h when kept at 0 °C. The gel became a partial gel when warmed up to 25 °C, and upon further heating at 120 °C for 20 min, the reverse reaction occurred. Therefore, the photogelation was repeatable.

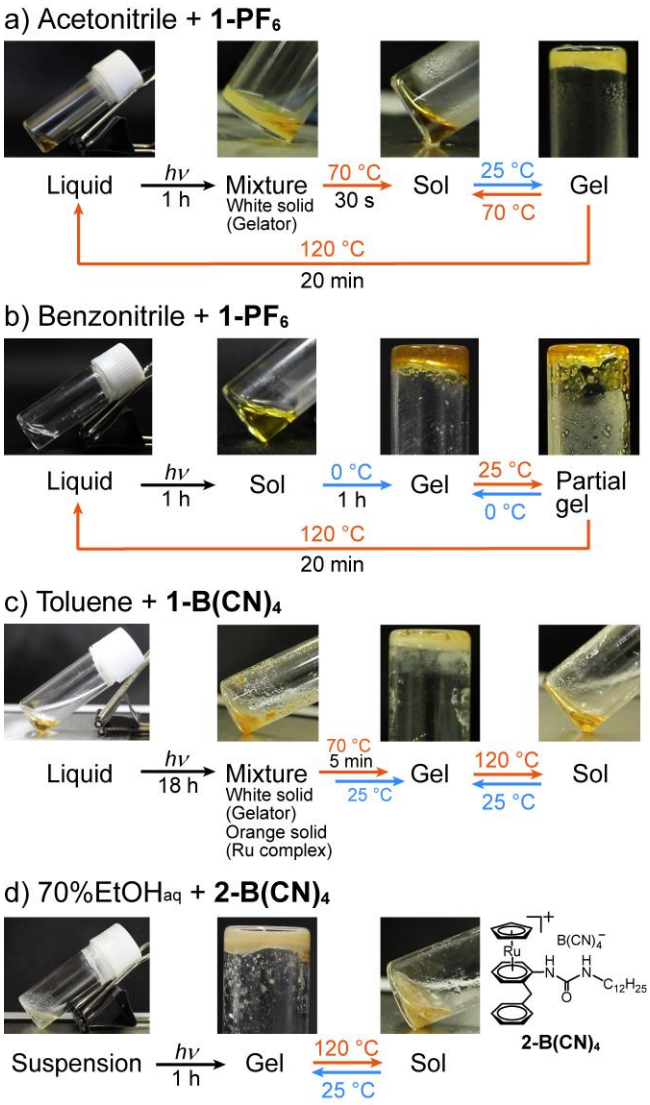

Fig. 6. Photographs of (a) acetonitrile (containing 5 wt.% **1-PF$_6$**), (b) benzonitrile (containing 5 wt.% **1-PF$_6$**), (c) toluene (containing 5 wt.% **1-B(CN)$_4$**), and (d) 70% ethanol aqueous solution (containing 5 wt.% **2-B(CN)$_4$**) before and after photoirradiation and after heating the photoproducts. The structure of **2-B(CN)$_4$** is also shown in (d).

A toluene solution containing 5 wt.% **1-PF$_6$** did not release the gelator upon photoirradiation due to the absence of coordinating sites, resulting in partial deposition the gelator. In contrast, a toluene solution containing 5 wt.% **1-B(CN)$_4$** underwent gelator release after 18 h of photoirradiation, resulting in the deposition of a white solid of gelator **L** and an orange solid of the anion-coordinated Ru complex. Although it was a mixture, it transformed to a gel after heating to 70 °C and being subsequently left at 25 °C for 1 h (Fig. 6c). Upon further heating the gel at 120 °C, toluene coordinated to the Ru complex to give a sandwich complex [CpRu(toluene)]$^+$, which was soluble in toluene. The gelator did not coordinate to the complex, hence only gel–sol transitions were repeatedly observed upon temperature changes of the resultant gel. Other nonpolar liquids such as liquid paraffin can be gelated with gelator **L**, although their photogelation with **1-B(CN)$_4$** was not possible because they were immiscible.

The gelation capability could be modulated by changing the ligand species. In addition to gelator **L**, there are many similar gelators with different gelation properties;[44] hence, appropriate gelators can be chosen. For example, gelator **L** is insoluble in a 70% ethanol aqueous solution and does not form a gel. However, gelator **L'** (= *o*-$C_6H_4(CH_2Ph)(NHCONHC_{12}H_{25})$) containing a benzyl group can gelate the liquid,[44] and photogelation was possible by using an **L'**-coordinated complex (**2-B(CN)$_4$**, Fig. 6d). The complex formed a suspension in the 70% ethanol aqueous solution although it formed a gel upon photoirradiation. After photogelation, only gel–sol transitions were repeatable upon temperature changes, because the photogenerated Ru complex decomposes in the solution. The results demonstrate that the photogelation capability of the complex can be adjusted by choosing the appropriate ligand species.

Crystal Structure of 1-PF$_6$

To investigate the intermolecular interactions in the gelator-coordinated complex, single-crystal X-ray analysis of **1-PF$_6$** was performed at −183 °C. The salt crystallized in space group *P*-1 (*Z* = 4) with two cation–anion pairs per asymmetric unit (Fig. 7). The Cp ring of cation **B** exhibited a two-fold rotational disorder (occupancy 0.57:0.43). The alkyl chains of cations **A** and **B** adopted linear and bent conformations, respectively (Fig. S12, ESI†), and the chains were arranged in parallel to form a layered structure. There were intermolecular hydrogen bonds (–N···O= distances: 2.91, 2.93 Å) between cations **A** and **B**, forming a one-dimensional chain. There was a π–π interaction between the Cp rings of cation **B** (interplanar distance 3.35 Å), with no other significant π–π interactions. In LMWGs with phenyl substituents, fiber structures are typically formed via π–π

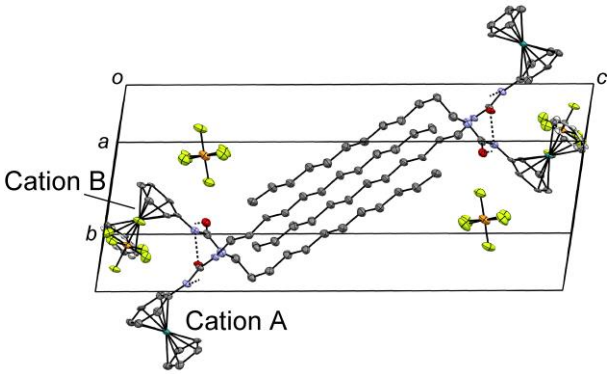

Fig. 7. Packing diagram of **1-PF$_6$** (−183 °C). Intermolecular -NH···O= hydrogen bonds are shown by dotted lines. Disordered parts are shown in gray.

stacking and hydrogen bond interactions.[5,6,46] There are organometallic gelators with planar molecular structures that can gelate ILs.[65] The structural analysis results suggest that the lack of gelation capability of **1-X** is ascribed to the presence of the bulky CpRu unit, which inhibits the π–π interaction.

Conclusions

We developed a simple, on-demand photogelation method for ILs using ionic liquid additives that release LMWGs upon photoirradiation. The compounds we designed are a novel class of photoresponsive gelators containing organometallic moieties, which are easy to synthesize and miscible with ILs. By adding a small amount of the compound, various ILs were transformed into ionogels upon UV photoirradiation, and the ionogel liquefied again upon heating owing to the thermal reverse reaction. The photogelation reaction was repeatable for ILs with coordinating cations. The photogelation conditions can be modified by choosing the ligands and anions, and several organic solvents were also photogelated. This is a simple and versatile method for the preparation of stimuli-responsive ionogels, and using this method, ILs can be immobilized or patterned after coating, printing, or filling; hence, this method may be useful for electronic device fabrication and micro-engineering applications. However, the photogelation time observed in the current study was too long, and the use of a high-power light source and improved molecular design may be needed for practical applications. For example, the utilization of coordinating substituents other than the cyano group may lead to improved performance, which is worthy of future investigation. This study has demonstrated that the use of photoreactive organometallic compounds is an effective strategy for manipulating supramolecular gels, which may expand the scope and applications of stimuli-responsive gels.

Author Contributions

R. Sumitani designed and conducted the experiments. M. Yamanaka synthesized the low-molecular-weight gelators and helped discussion. T. Mochida conceived and directed the project. R. Sumitani and T. Mochida wrote the manuscript.

Conflicts of interest

The authors declare no conflict of interest.

Acknowledgements

This work was supported financially by KAKENHI (grant numbers: 20H02756 (T.M.), 17H06374 (M.Y.), and 21K06485 (M.Y.)) from the Japan Society for the Promotion of Science (JSPS) and Grant-in-Aid for JSPS Research Fellow (grant number: 21J12056 (R.S.)).

Notes and references

1 E. R. Draper and D. J. Adams, *Chem*, 2017, **3**, 390–410.
2 P. Terech and R. G. Weiss, *Chem. Rev.*, 1997, **97**, 3133–3160.
3 S. S. Babu, V. K. Praveen and A. Ajayaghosh, *Chem. Rev.*, 2014, **114**, 1973–2129.
4 J. Le Bideau, L. Viau and A. Vioux, *Chem. Soc. Rev.*, 2011, **40**, 907–925.
5 P. Dastidar, *Chem. Soc. Rev.*, 2008, **37**, 2699–2715.
6 M. de Loos, B. L. Feringa and J. H. van Esch, *Eur. J. Org. Chem.*, 2005, **2005**, 3615–3631.
7 N. Thakur, B. Sharma, S. Bishnoi, S. K. Mishra, D. Nayak, A. Kumar and T. K. Sarma, *ACS Sustainable Chem. Eng.*, 2018, **6**, 8659–8671.
8 H. Sawalha, R. den Adel, P. Venema, A. Bot, E. Flöter and E. van der Linden, *J. Agric. Food Chem.*, 2012, **60**, 3462–3470.
9 Y. Nishida, A. Tanaka, S. Yamamoto, Y. Tominaga, N. Kunikata, M. Mizuhata and T. Maruyama, *Angew. Chem. Int. Ed.*, 2017, **56**, 9410–9414.
10 S. Ray, A. K. Das and A. Banerjee, *Chem. Mater.*, 2007, **19**, 1633–1639.
11 B. Adhikari, G. Palui and A. Banerjee, *Soft Matter*, 2009, **5**, 3452–3460.
12 M. O. Guler and S. I. Stupp, *J. Am. Chem. Soc.*, 2007, **129**, 12082–12083.
13 N. Singh, M. Tena-Solsona, J. F. Miravet and B. Escuder, *Isr. J. Chem.*, 2015, **55**, 711–723.
14 T. Tu, W. Assenmacher, H. Peterlik, R. Weisbarth, M. Nieger and K. H. Dötz, *Angew. Chem. Int. Ed.*, 2007, **46**, 6368–6371.
15 Z. Li, Y. Zhou, T. Li, J. Zhang and H. Tian, *VIEW.*, 2021, 20200112.
16 K. J. Skilling, F. Citossi, T. D. Bradshaw, M. Ashford, B. Kellam and M. Marlow, *Soft Matter*, 2014, **10**, 237–256.
17 E. R. Draper and D. J. Adams, *Chem. Commun.*, 2016, **52**, 8196–8206.
18 R. Ochi, T. Nishida, M. Ikeda and I. Hamachi, *J. Mater. Chem. B*, 2014, **2**, 1464–1469.
19 M. Ikeda, R. Ochi, Y. Kurita, D. J. Pochan and I. Hamachi, *Chem. Eur. J.*, 2012, **18**, 13091–13096.
20 S.-L. Zhou, S. Matsumoto, H.-D. Tian, H. Yamane, A. Ojida, S. Kiyonaka and I. Hamachi, *Chem. Eur. J.*, 2005, **11**, 1130–1136.
21 Q. Chen, D. Zhang, G. Zhang and D. Zhu, *Langmuir*, 2009, **25**, 11436–11441.
22 Q. Chen, Y. Lv, D. Zhang, G. Zhang, C. Liu and D. Zhu, *Langmuir*, 2010, **26**, 3165–3168.
23 J. Gao, J. Zhan and Z. Yang, *Adv. Mater.*, 2020, **32**, 1805798.
24 H. He, W. Tan, J. Guo, M. Yi, A. N. Shy and B. Xu, *Chem. Rev.*, 2020, **120**, 9994–10078.

25 I. Tomatsu, K. Peng and A. Kros, *Adv. Drug Deliv. Rev.*, 2011, **63**, 1257–1266.
26 W. Fang, X. Liu, Z. Lu and T. Tu, *Chem. Commun.*, 2014, **50**, 3313–3316.
27 T. Muraoka, C.-Y. Koh, H. Cui and S. I. Stupp, *Angew. Chem. Int. Ed.*, 2009, **48**, 5946–5949.
28 X. Zheng, Q. Miao, W. Wang and D.-H. Qu, *Chin. Chem. Lett.*, 2018, **29**, 1621–1624.
29 P. J. Jervis, L. Hilliou, R. B. Pereira, D. M. Pereira, J. A. Martins and P. M. T. Ferreira, *Nanomaterials*, 2021, **11**, 704.
30 D. Koda, T. Maruyama, N. Minakuchi, K. Nakashima and M. Goto, *Chem. Commun.*, 2010, **46**, 979–981.
31 A. Tanaka, Y. Fukuoka, Y. Morimoto, T. Honjo, D. Koda, M. Goto and T. Maruyama, *J. Am. Chem. Soc.*, 2015, **137**, 770–775.
32 Z. Yang, G. Liang and B. Xu, *Acc. Chem. Res.*, 2008, **41**, 315–326.
33 Z. Yang, G. Liang, L. Wang and B. Xu, *J. Am. Chem. Soc.*, 2006, **128**, 3038–3043.
34 D.-Z. Zhang, Y.-Y. Ren, Y. Hu, L. Li and F. Yan, *Chinese J. Polym. Sci.*, 2020, **38**, 506–513.
35 X. Liu, B. He, Z. Wang, H. Tang, T. Su and Q. Wang, *Sci. Rep.*, 2014, **4**, 6673.
36 E. Kamio, M. Minakata, Y. Iida, T. Yasui, A. Matsuoka and H. Matsuyama, *Polym. J.*, 2020, **53**, 137–147.
37 M. Kar, K. Matuszek and D. R. MacFarlane, *Ionic Liquids in Kirk-Othmer Encyclopedia of Chemical Technology*, Wiley, Hoboken, 2019.
38 T. Ueki, Y. Nakamura, R. Usui, Y. Kitazawa, S. So, T. P. Lodge and M. Watanabe, *Angew. Chem. Int. Ed.*, 2015, **54**, 3018–3022.
39 T. Ueki, R. Usui, Y. Kitazawa, T. P. Lodge and M. Watanabe, *Macromolecules*, 2015, **48**, 5928–5933.
40 H. Mizuno, K. Hashimoto, K. Shigenobu, H. Kokubo, K. Ueno and M. Watanabe, *Macromol. Rapid Commun.*, 2021, **42**, 2100091.
41 L. Wang, X. Ma, L. Wu, Y. Sha, B. Yu, X. Lan, Y. Luo, Y. Shi, Y. Wang and Z. Luo, *Eur. Polym. J.*, 2021, **144**, 110213.
42 R. Tamate, R. Usui, K. Hashimoto, Y. Kitazawa, H. Kokubo and M. Watanabe, *Soft Matter*, 2018, **14**, 9088–9095.
43 X. Ma, R. Usui, Y. Kitazawa, R. Tamate, H. Kokubo and M. Watanabe, *Macromolecules*, 2017, **50**, 6788–6795.
44 T. Komiyama, Y. Harada, T. Hase, S. Mori, S. Kimura, M. Yokoya and M. Yamanaka, *Chem. Asian J.*, 2021, **16**, 1750–1755.
45 M. Yamanaka and N. Miyachi, *WO Pat.*, WO2017099232A1, 2017.
46 F. Piana, D. H. Case, S. M. Ramalhete, G. Pileio, M. Facciotti, G. M. Day, Y. Z. Khimyak, J. Angulo, R. C. D. Brown and P. A. Gale, *Soft Matter*, 2016, **12**, 4034–4043.
47 T. P. Gill and K. R. Mann, *Organometallics*, 1982, **1**, 485–488.
48 B. M. Trost and C. M. Older, *Organometallics*, 2002, **21**, 2544–2546.
49 Y. Funasako, S. Mori and T. Mochida, *Chem. Commun.*, 2016, **52**, 6277–6279.
50 T. Ueda,T. Tominaga, T. Mochida, K. Takahashi and S. Kimura, *Chem. Eur. J.*, 2018, **24**, 9490–9493.
51 R. Sumitani, H. Yoshikawa and T. Mochida, *Chem. Commun.*, 2020, **56**, 6189–6192.
52 R. Sumitani and T. Mochida, *Macromolecules*, 2020, **53**, 6968–6974.
53 R. Sumitani and T. Mochida, *Soft Matter*, 2020, **16**, 9946–9954.
54 O. Kuzmina, N. H. Hassan, L. Patel, C. Ashworth, E. Bakis, A. J. P. White, P. A. Hunt and T. Welton, *Dalton Trans.*, 2017, **46**, 12185–12200.
55 S. M. Mahurin, P. C. Hillesheim, J. S. Yeary, D.-E. Jiang and S. Dai, *RSC Adv.*, 2012, **2**, 11813–11819.
56 G. M. Sheldrick, *Acta Cryst. A*, 2008, **64**, 112–122.
57 T. Küppers, E. Bernhardt, H. Willner, H. W. Rohm and M. Köckerling, *Inorg. Chem.*, 2005, **44**, 1015–1022.
58 Z. Fei, D. Zhao, D. Pieraccini, W. H. Ang, T. J. Geldbach, R. Scopelliti, C. Chiappe and P. J. Dyson, *Organometallics*, 2007, **26**, 1588–1598.
59 D. Zhao, Z. Fei, T. J. Geldbach, R. Scopelliti and P. J. Dyson, *J. Am. Chem. Soc.*, 2004, **126**, 15876–15882.
60 N. Amiri, H. Benyounes, Z. Lounis and W. Shen, *Chem. Eng. Res. Des.*, 2021, **169**, 239–249.
61 X. Zhang, X. Feng, H. Li, J. Peng, Y. Wu and X. Hu, *Ind. Eng. Chem. Res.*, 2016, **55**, 11012–11021.
62 S. Debnath, A. Shome, S. Dutta, P. K. Das, *Chem. Eur. J.* 2008, **14**, 6870–6881.
63 D. Ghosh, M. T. Mulvee and K. K. Damodaran, *Molecules*, 2019, **24**, 3472.
64 M. Sun, H. Sun, Y. Wang, M. Sánchez-Soto and D. A. Schiraldi, *Gels*, 2018, **4**, 33.
65 T. Tu, X. Bao, W. Assenmacher, H. Peterlik, J. Daniels, K.H. Dötz, *Chem. Eur. J.*, 2009, **15**, 1853–1861.

TOC

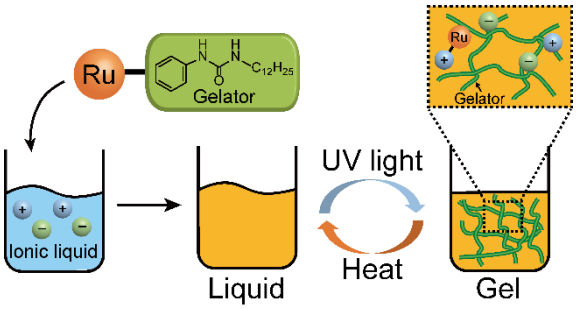

We developed organometallic complexes that release low-molecular-weight gelators upon UV photoirradiation; various ionic liquids can be photogelated by using them.

Supporting Information

On-demand Gelation of Ionic Liquids Using Photoresponsive Organometallic Gelators

Ryo Sumitani,[a] Masamichi Yamanaka [b] and Tomoyuki Mochida *[a,c]

[a]*Department of Chemistry, Graduate School of Science, Kobe University, 1-1 Rokkodai, Nada, Kobe, Hyogo 657-8501, Japan. E-mail: tmochida@platinum.kobe-u.ac.jp*

[b]*Meiji Pharmaceutical University, 2-522-1 Noshio, Kiyose, Tokyo 204–8588, Japan*

[c]*Research Center for Membrane and Film Technology, Kobe University, 1-1 Rokkodai, Nada, Kobe, Hyogo 657-8501, Japan*

Contents

Experimental

Synthesis of $[C_6CNEt_3N][Tf_2N]$

Synthesis of [CpRu(**L'**)][$B(CN)_4$] (**2-$B(CN)_4$**)

Figures and Tables

Fig. S1. DSC curve of **1-PF_6**.

Fig. S2. FT-IR and ^{1}H NMR (CD_3CN) spectra of **1-PF_6**, **1-$B(CN)_4$**, and **L**.

Fig. S3. Photographs of **C** and **D**.

Fig. S4. ^{1}H NMR spectra (CD_3CN) of **B**–**E**.

Fig. S5. FT-IR spectra of **A**, **B**, **D**, and **E**.

Fig. S6. DSC curves of the ionogels.

Fig. S7. SEM images of the ionogels.

Fig. S8. Viscoelastic moduli and complex viscosity of the ionogels.

Fig. S9. Storage modulus and loss modulus of the ionogels.

Fig. S10. Viscoelastic moduli and complex viscosity of the ionogels.

Fig. S11. Viscoelastic moduli and complex viscosity of the ionogels.

Fig. S12. Molecular structures of the cations of **1-PF$_6$** in the crystal.

Fig. S13. TG-DTA curves of gelator **L**.

Table S1. Crystallographic parameters.

Table S2. Gel-sol transition temperature of the ionogels.

Experimental

Synthesis of [C_6CNEt_3N][Tf_2N]. In a nitrogen atmosphere, an amount of 7-bromoheptanenitrile (1.84 g, 9.7 mmol) was slowly added to a solution of triethylamine (1.0 g, 9.88 mmol) in acetonitrile (2 mL). The solution was subsequently heated at 80 °C for 3 h with constant stirring. The solvent was then removed under reduced pressure. The resultant orange liquid was washed 10 times with hexane and dried under vacuum at 80 °C for 1 h to obtain [C_6CNEt_3N]Br as an orange liquid (2.5 g, 90%). Potassium bis(trifluoromethanesulfonyl)imide (KTf_2N; 6.2 g, 19.4 mmol) was added to an aqueous solution (20 mL) of [C_6CNEt_3N]Br (2.5 g, 8.7 mmol), and the solution was stirred vigorously for 1 h. The resultant [C_6CNEt_3N][Tf_2N] phase was collected and washed three times with water. The orange liquid was dried under vacuum for 3 h at 60 °C. The crude product was purified by column chromatography (alumina, eluent: dichloromethane/acetonitrile, gradient from 1:0 to 0:1). After evaporation of the solvent, the residue was dissolved in acetonitrile and heated to reflux, to which a small amount of activated carbon was added. The activated carbon was then removed by filtration without cooling. After evaporation of the solvent, the residue was dried under vacuum at 130 °C for 6 h. The desired product was a pale-yellow liquid (3.4 g, 69% yield). T_g = −72 °C (DSC). ^{1}H NMR (400 MHz, $CDCl_3$): δ = 1.35 (t, 9H, $N(CH_2CH_3)_3$, J = 7.22 Hz), 1.46 (m, 2H, $NC_3H_6CH_2$), 1.56 (m, 2H, $NC_2H_4CH_2$), 1.70 (m, 4H, $NCH_2CH_2C_2H_4CH_2$), 2.39 (t, 2H, $NC_5H_{10}CH_2$, J = 6.89 Hz), 3.16 (t, 2H, NCH_2, J = 8.51 Hz), 3.29 (q, 6H, $N(CH_2CH_3)_3$). FT-IR (ATR, cm^{-1}): 600, 613, 653, 739, 761, 1052 (S=O), 1134, 1177 (C–F), 1330, 1348, 1397, 1460, 1487, 2246 (CN), 2869 (C–H), 2950 (C–H). Anal. Calcd. for $C_{15}H_{27}F_6N_3O_4S_2$: C, 36.66, H, 5.54, N, 8.55. Found: C, 36.48, H, 5.72, N, 8.38.

Synthesis of [CpRu(L')][$B(CN)_4$] (2-$B(CN)_4$). [CpRu(**L'**)]PF_6 (**2-PF_6**) was synthesized using the procedure identical to that for **1-PF_6** using **L'** (33 mg, 0.083 mmol) and [$CpRu(CH_3CN)_3$]PF_6 (30 mg, 0.069 mmol). The desired product was obtained as an orange viscous liquid (27 mg, 55%). ^{1}H NMR (400 MHz, $CDCl_3$): δ = 0.88 (t, 3H, CH_3, J = 6.89 Hz), 1.26 (m,

18H, $NHC_2H_4C_9H_{18}$), 1.58 (m, 2H, $NHCH_2CH_2$), 3.21 (m, 2H, $NHCH_2$), 4.00 (m, 2H, $PhCH_2$), 5.26 (s, 5H, Cp-*H*), 5.60–5.88 (m, 4H, Ru–Ph–*H*), 6.98 (s, 1H, $NHC_{12}H_{25}$), 7.22 (s, 1H, PhN*H*), 7.10–7.40 (m, 5H, CH_2Ph-*H*). FT-IR (ATR, cm^{-1}): 567 (P–F), 745, 1242, 1289, 1451 (Cp, C=C), 1465, 1482, 1563 (Arene, C=C), 1632 (C=O), 2847, 2916 (C–H). **2-B(CN)$_4$** was synthesized using the procedure identical to that for **1-B(CN)$_4$** using **2-PF$_6$** (21 mg, 0.030 mmol) and $KB(CN)_4$ (14 mg, 0.089 mmol). The desired product was obtained as an orange viscous liquid (13 mg, 65% yield). ^{1}H NMR (400 MHz, $CDCl_3$): δ = 0.88 (t, 3H, CH_3, J = 6.89 Hz), 1.26 (m, 18H, $NHC_2H_4C_9H_{18}$), 1.58 (m, 2H, $NHCH_2CH_2$), 3.21 (m, 2H, $NHCH_2$), 4.00 (m, 2H, $PhCH_2$), 5.26 (s, 5H, Cp-*H*), 5.60–5.88 (m, 4H, Ru–Ph–*H*), 6.98 (s, 1H, $NHC_{12}H_{25}$), 7.22 (s, 1H, PhN*H*), 7.10–7.40 (m, 5H, CH_2Ph-*H*).

Figures and Tables

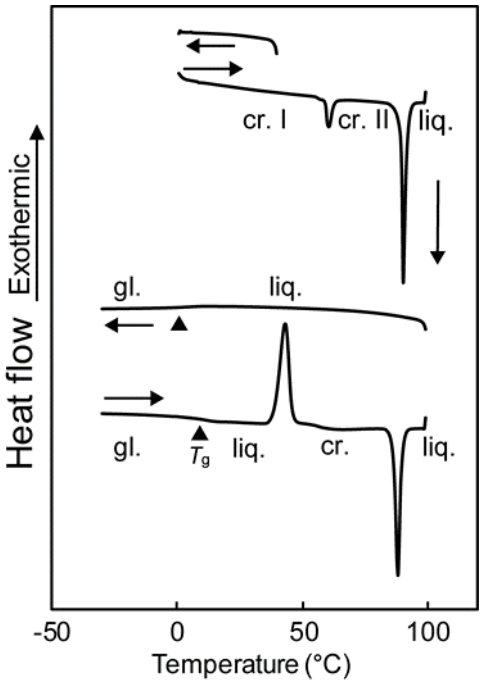

Fig. S1. DSC curve of **1-PF$_6$**, where cr., liq,. and gl. are the crystal, liquid, and glassy states, respectively. A cold-crystallization peak is seen at 45 °C in the second cycle.

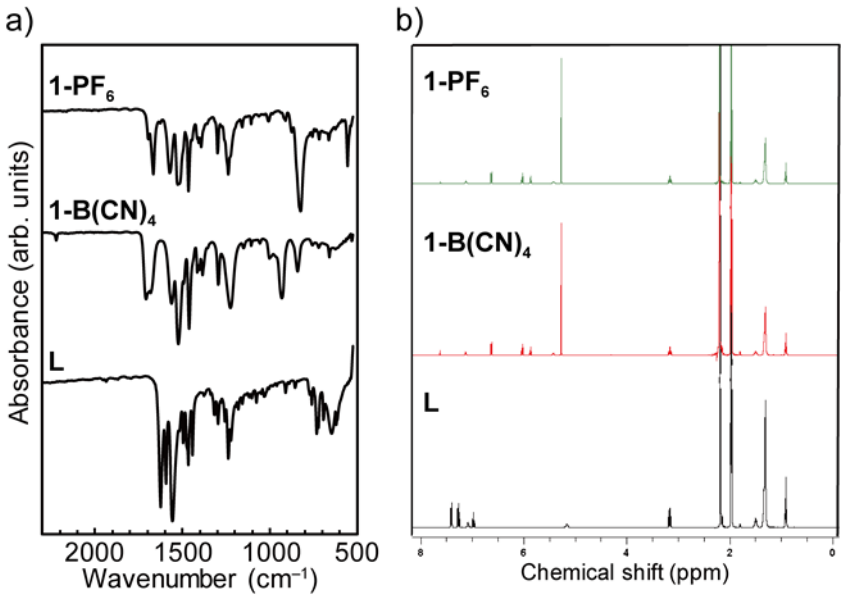

Fig. S2. (a) FT-IR and (b) ^{1}H NMR (CD_3CN) spectra of **1-PF$_6$**, **1-B(CN)$_4$**, and **L**.

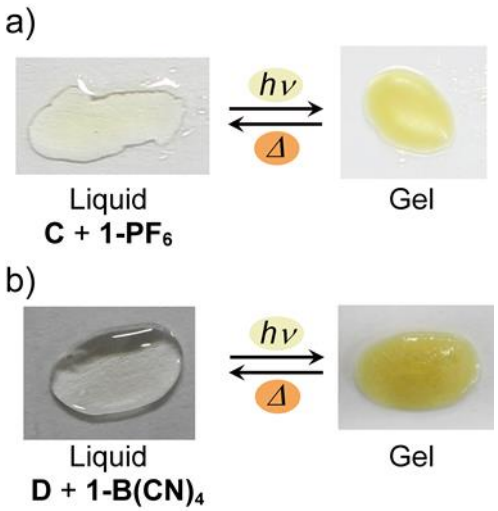

Fig. S3. Photographs of **C** (containing 5 wt.% **1-PF$_6$**) and **D** (containing 5 wt.% **1-B(CN)$_4$**) before and after photoirradiation.

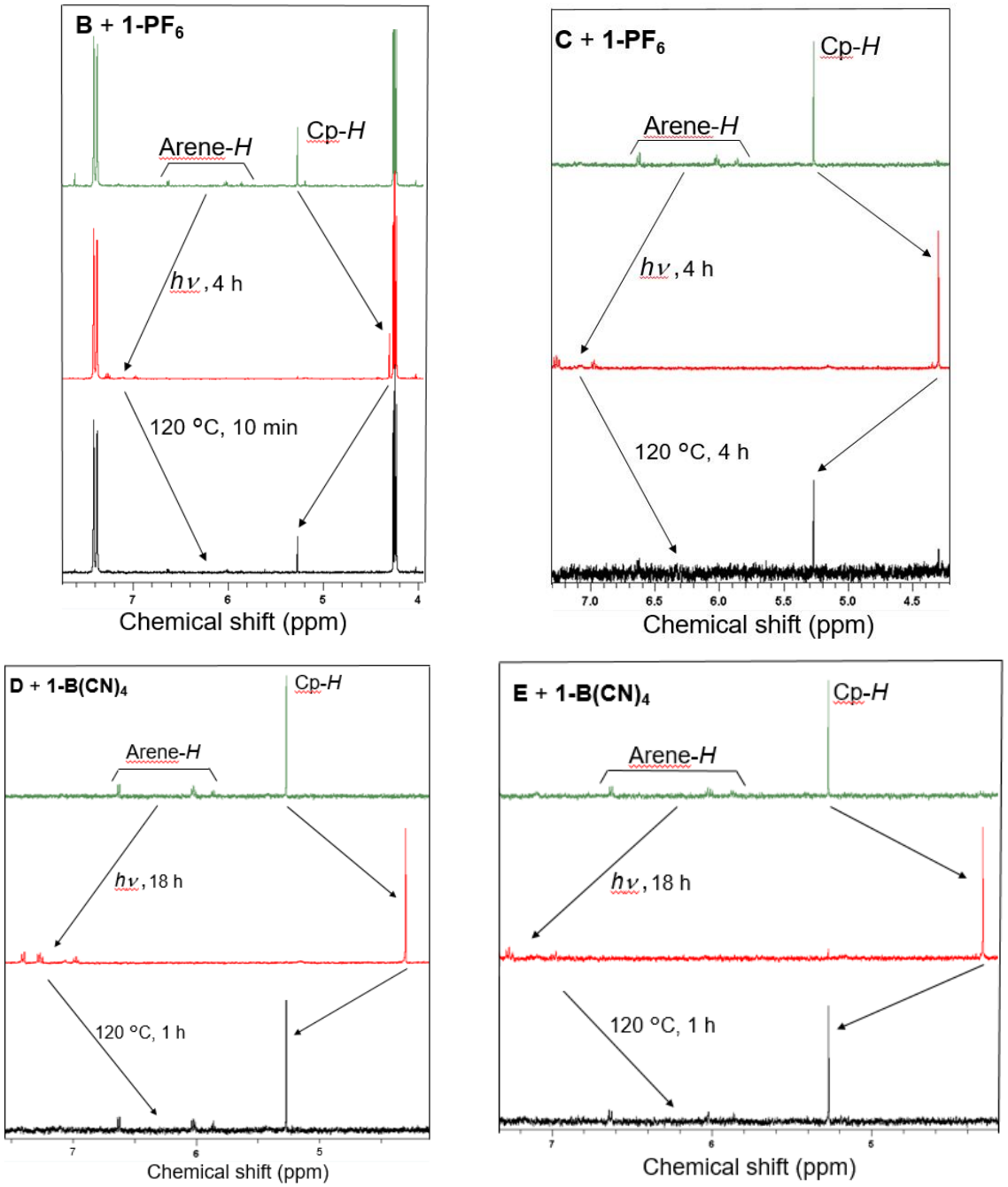

Fig. S4. ^{1}H NMR spectra (CD_3CN) of **B**–**E** (containing 5 wt.% **1-X**) before and after photoirradiation and subsequent heating at 120 °C.

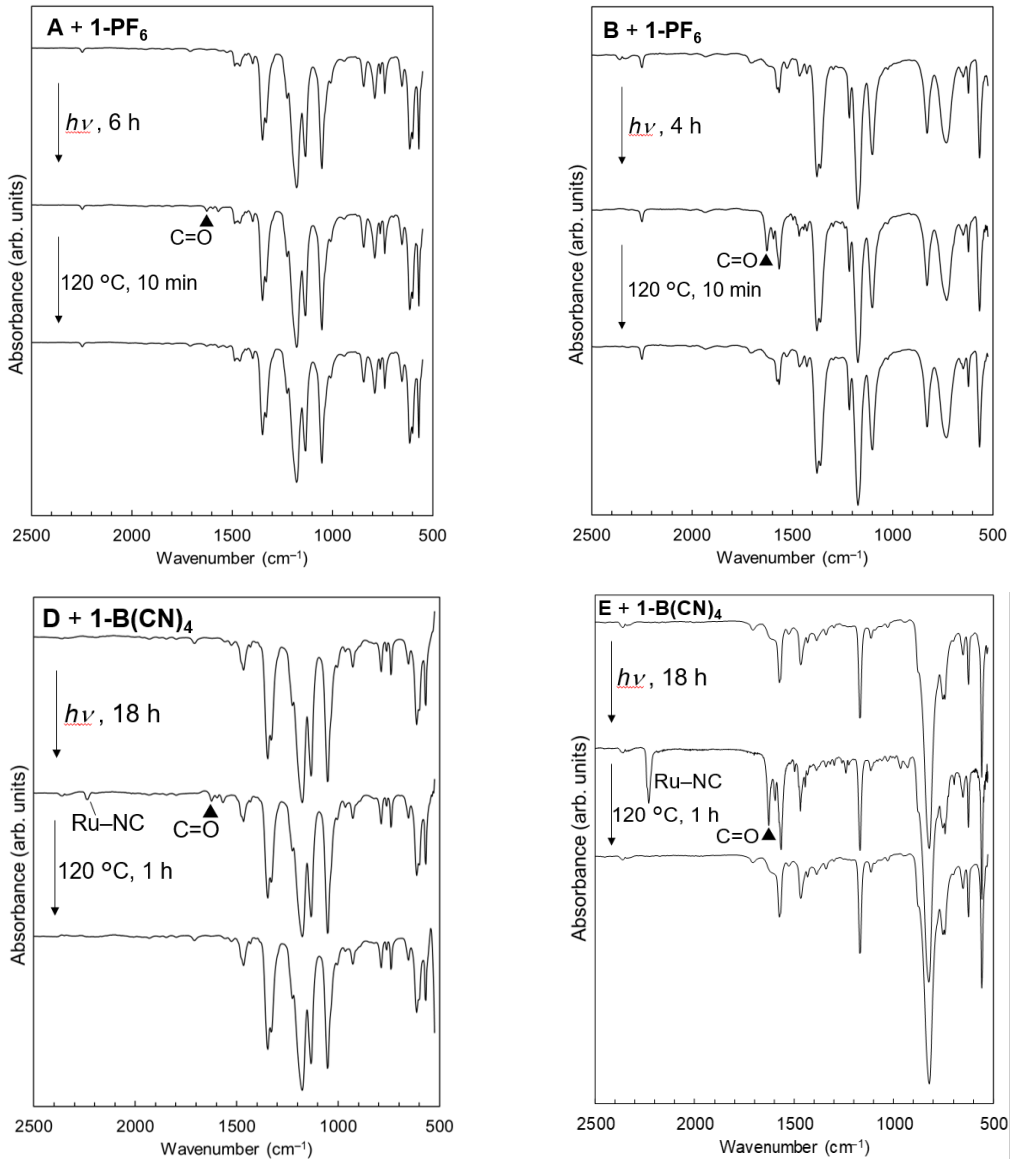

Fig. S5. FT-IR spectra of **A**, **B**, **D**, and **E** (containing 5 wt.% **1-X**) before and after photoirradiation and after subsequent heating at 120 °C.

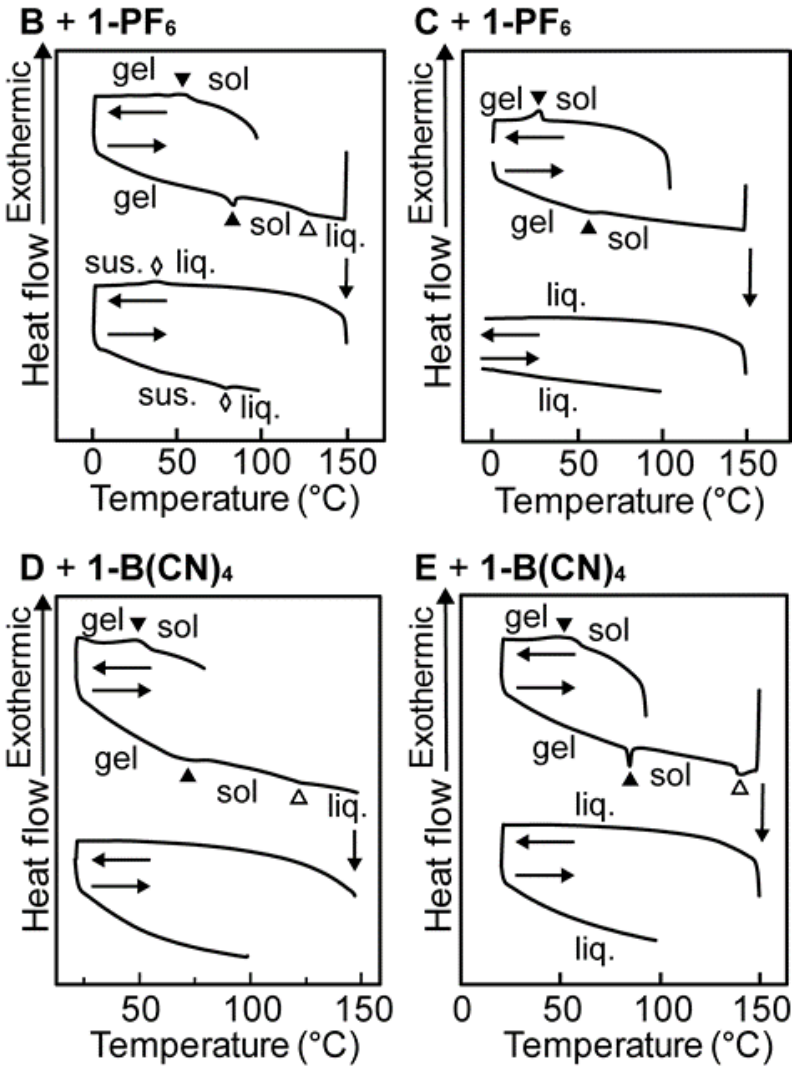

Fig. S6. DSC curves of the ionogels prepared by photoirradiation of **B–E** (containing 5 wt.% **1-X**), where liq. and sus. are the liquid and suspension states, respectively. The peaks corresponding to the gel–sol transition, gelator coordination, and dissolution of the complex are shown by ▲, △, and ◊ symbols, respectively.

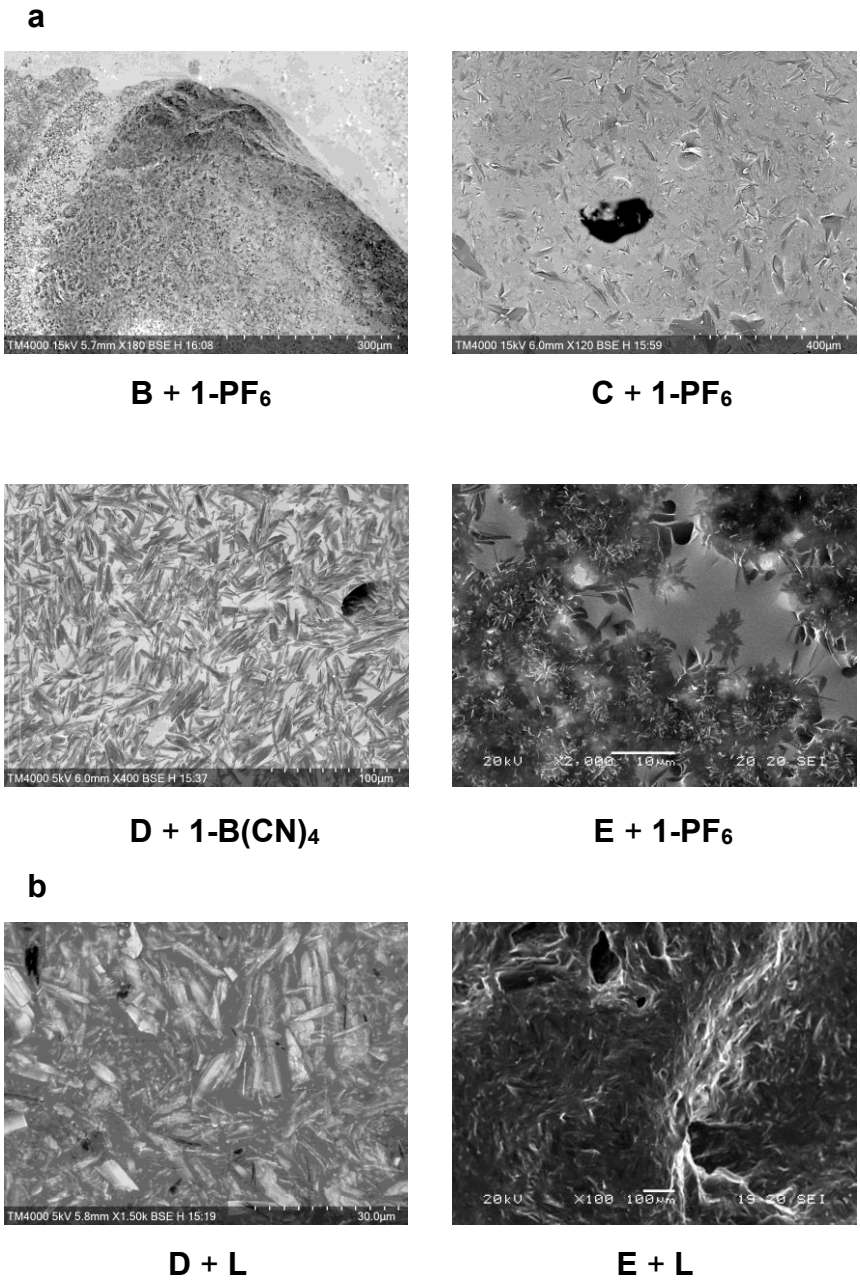

Fig. S7. SEM images of the ionogels prepared by (a) photoirradiation of **B–E** (containing **1-X** 5 wt.%) and (b) addition of gelator **L** (2.4 wt.%) to the ILs. The dark spot in the right figure in (a) is an artifact by electron beam damage.

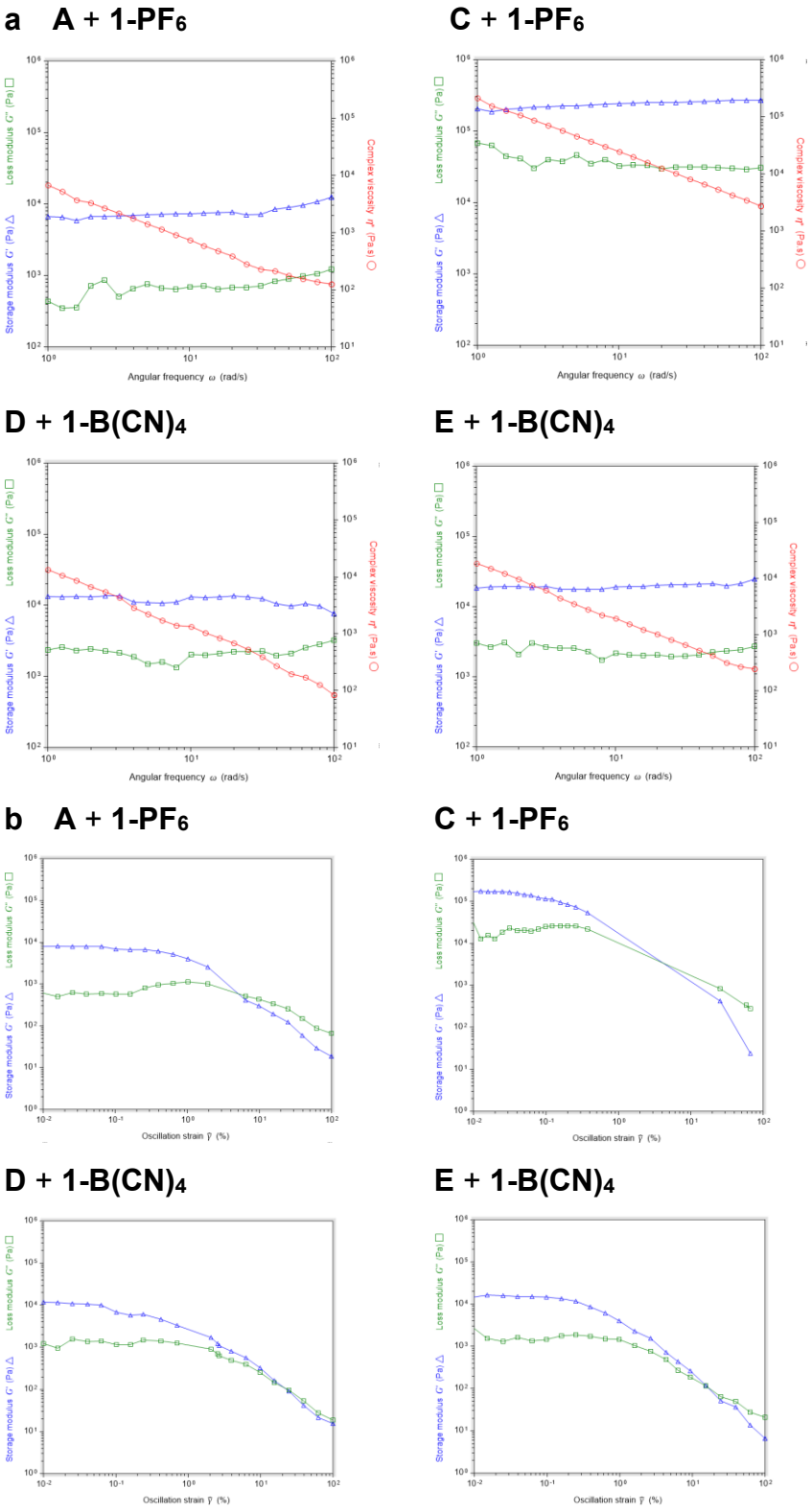

Fig. S8. (a) Angular frequency dependence (25 °C, strain 0.1%) and (b) strain dependence (10 rad s^{-1}) of viscoelastic moduli (G': △, G'': □) and complex viscosity (○) of the ionogels prepared by the photoirradiation of **A**, **B**, **D**, and **E** (containing 5 wt.% **1-X**). Data for **A** and **C** are acquired after thermal treatment (100 °C, 30 s).

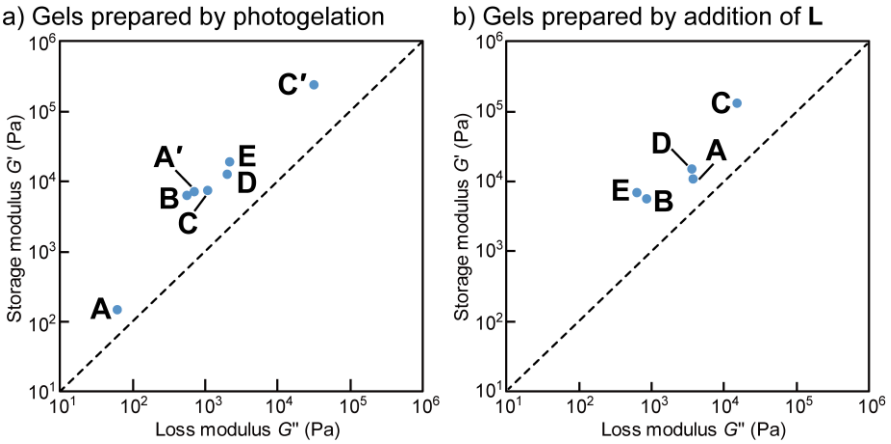

Fig. S9. Plots of storage modulus (G') and loss modulus (G'') of the ionogels prepared by the (a) photoirradiation of **A**–**E** (containing 5 wt.% **1-X**) and (b) addition of gelator **L** (**A**–**C**: 2.4 wt.%, **D** and **E**: 2.5 wt.%) to the ILs. For **A** and **C**, the values after thermal treatment of the gel (100 °C, 30 s) are also plotted (**A′** and **C′**).

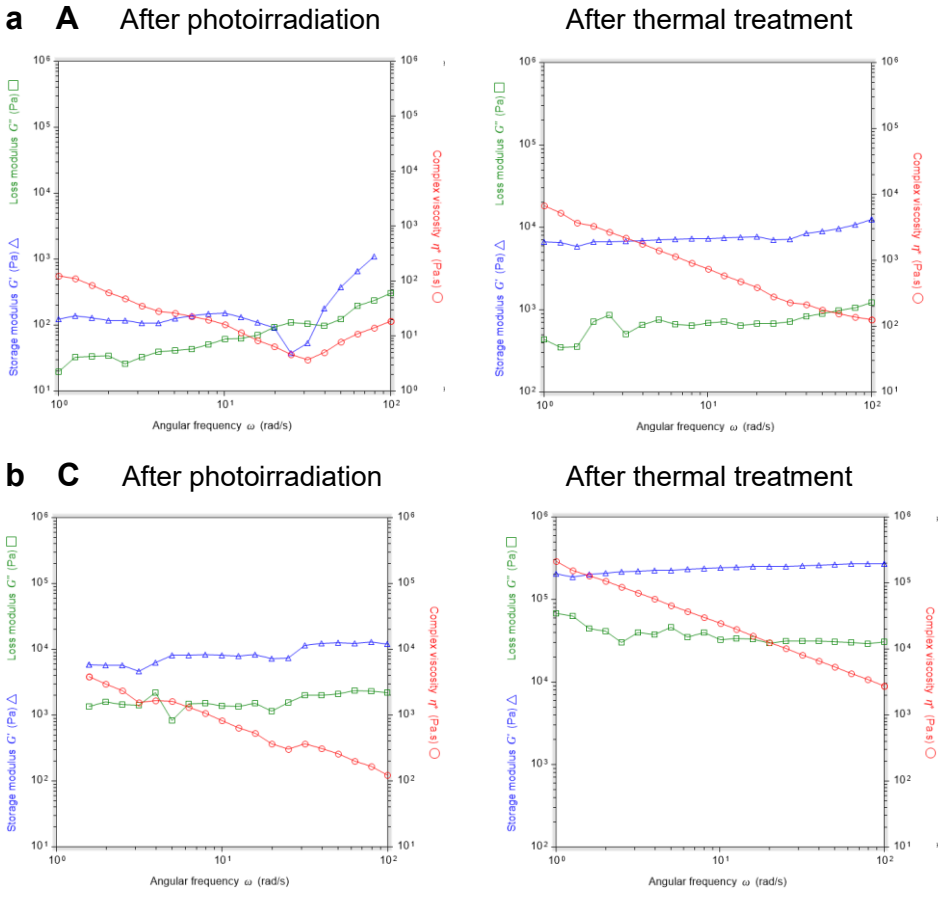

Fig. S10. Angular frequency dependence (25 °C, strain 0.1%) of the viscoelastic moduli (G': △, G'': □) and complex viscosity (○) of gels of (a) **A** and (b) **C** (containing 5 wt.% **1-PF$_6$**) formed upon photoirradiation. Data acquired immediately after photoirradiation (left) and after subsequent thermal treatment (100 °C, 30 s; right) are shown.

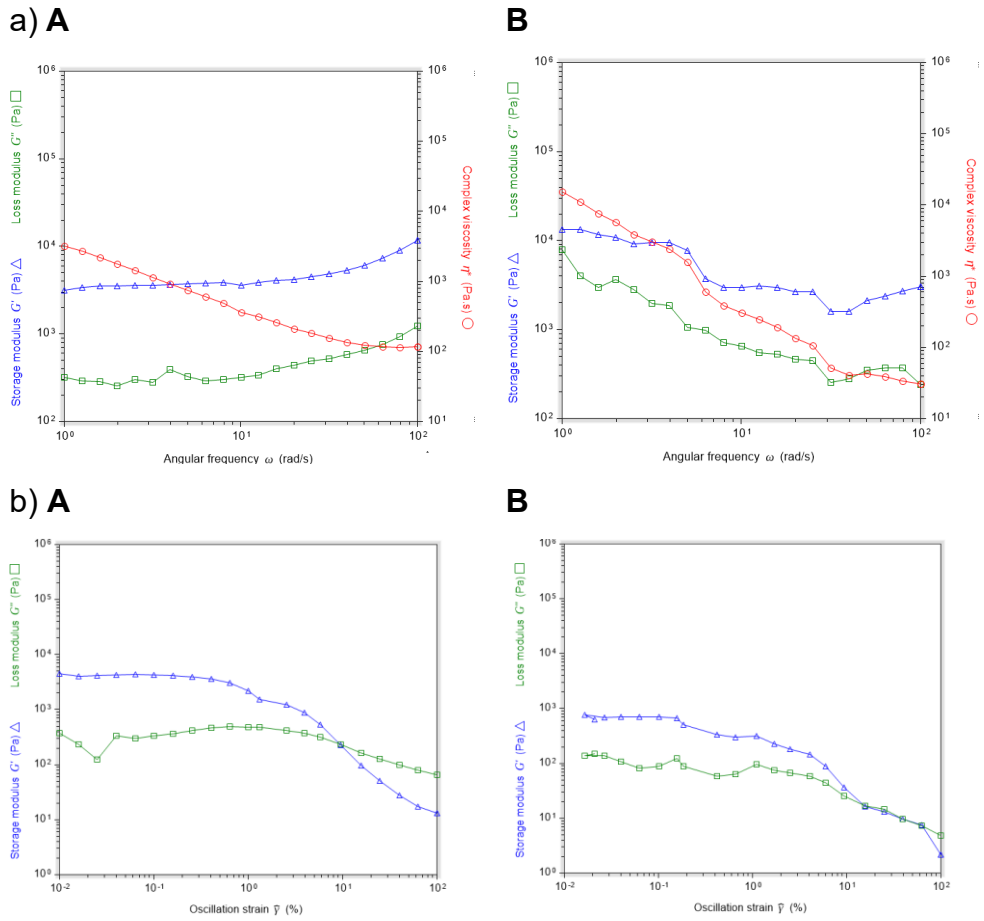

Fig. S11. (a) Angular frequency dependence (25 °C, strain 0.1%) and (b) strain dependence (10 rad s^{-1}) of the viscoelastic moduli (G': △, G'': □) and complex viscosity (○) of ionogels from **A** and **B** (containing 5 wt.% **1-PF$_6$**) after three cycles of photoirradiation. The data for **A** were acquired after thermal treatment (100 °C, 30 s).

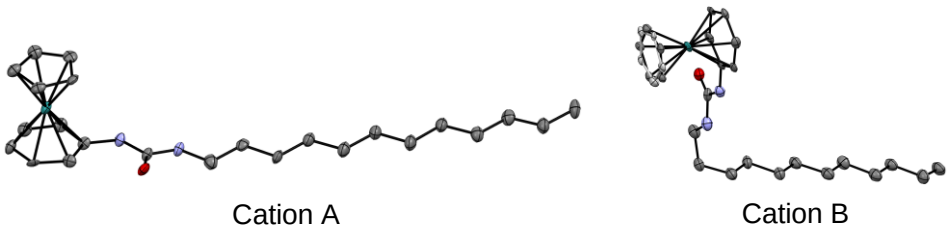

Fig. S12. Molecular structures of the cations of **1-PF$_6$** in the crystal (−183 °C). The disordered moieties of cation **B** are displayed in gray.

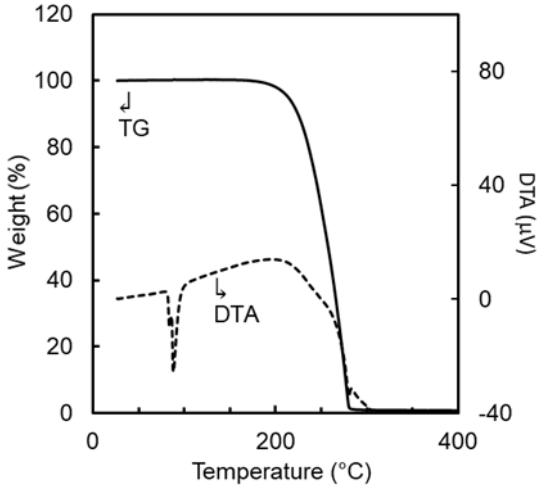

Fig. S13. TG-DTA curves of gelator **L** (10 °C min^{-1}, N_2 atmosphere). There is a melting peak in the DTA curve at around 90 °C.

Table S1. Crystallographic parameters.

	1-PF_6
Empirical formula	$C_{24}H_{37}F_6N_2OPRu$
Formula weight	615.59
Crystal system	triclinic
Space group	$P\bar{1}$
a [Å]	9.637(4)
b [Å]	9.944(5)
c [Å]	27.528(13)
α [°]	95.325(6)
β [°]	97.691(8)
γ [°]	96.476(6)
V [Å^3]	2582(2)
Z	4
ρ_{calcd} [g cm^{-3}]	1.584
μ [mm^{-1}]	0.733
Temperature [K]	90
F(000)	1264
Reflns collected	9148
R (int)	0.0363
Goodness of fit	1.098
$R_1{}^a$, $R_w{}^b$ ($I > 2\sigma$)	0.1041, 0.2448
$R_1{}^a$, $R_w{}^b$ (all data)	0.1393, 0.2643

$^aR_1 = \Sigma||F_o| - |F_c|| / \Sigma|F_o|$. $^bR_w = [\Sigma w (F_o^2 - F_c^2)^2 / \Sigma w (F_o^2)^2]^{1/2}$

Table S2. Gel–sol transition temperature of the ionogels prepared by adding gelator **L**.

IL	T_{gel} (°C)	
	heating	cooling
A[a]	70	41
B[a]	85	57
C[a]	61	33
D[b]	69	45
E[b]	84	47

The amount of gelator added: a) 2.4 wt.% and b) 2.5 wt.%.